ICAS 2016

30th Congress of the International Council of the Aeronautical Sciences
DCC, Daejeon, Korea ; September 25-30, 2016

NUMERICAL STUDY OF FIXED TRANSITION LOCATION EFFECT ON SUPERCRITICAL WING AERODYNAMIC CHARACTERISTICS

Qian Guangping1*, Si Jiangtao, Qin Xiaohui**, Zhongyuan****
***Shanghai Aircraft Design and Research Institute**

Keywords: *Fixed transition; Supercritical wing; Full-potential equation; Reynolds number;*

Abstract

Numerical simulations are performed to investigate the effect of fixed transition location on supercritical wing aerodynamic characteristics for transonic supercritical flows. The three-dimensional compressible full potential equations coupled with boundary-layer corrections are solved. Computational grids around wing/body/nacelles are built by algebraic methods. Solutions at both wind tunnel Reynolds number and flight Reynolds number are numerical computed, and are compared with high Reynolds number experimental data. The simulation results and high Reynolds number experimental data are quite similar, indicating the mesh quality and numerical methods are adequate in this study. The key point of this paper is the fixed transition location effect on pressure distribution, boundary layer thickness and lift-to-drag characteristics. Many numerical simulations are conducted over a range of parameters (Reynolds number, Mach number, etc). The numerical results indicate that the fixed transition location plays a significant role on aerodynamic characteristics of supercritical wing in wind tunnel test .The current numerical studies can give some useful guidance for low Reynolds number wind tunnel test to provide reliable and validated wind tunnel test data for the correction of Reynolds number effect.

1 General Introduction

A scaled-down model is often adopted in wind tunnel test. Therefore, the flow characteristics are different from full-scale configuration flows. The flows become turbulent from the leading edge of most components for a full-scale aircraft. As the wind tunnel Reynolds number is often low, to a certain extent there are some laminar flows in the scaled-down model if free transition is employed in the wind tunnel test. It experiences three different processes from low Reynolds number to high Reynolds number under the condition of free transition. There are absolutely laminar flows in low Reynolds number. Therefore, the interactions of laminar boundary layers with shock waves occur in transonic flow. There are laminar flows before shock waves and turbulent flow after shock waves in medium Reynolds number. Therefore, the interactions of boundary layers transition with shock waves occur. There are already full turbulent flows in high Reynolds number. Therefore, the interactions of turbulent boundary layers with shock waves occur. It is difficult to acquire the variation rule of aerodynamic characteristics with Reynolds number because of three different flow characteristics. Consequently, it is unable to correct the wind tunnel test data for Reynolds number effect to predict aerodynamic characteristics of flight conditions. Accordingly, fixed transition is often adopted by utilizing transition trips placed on the model to force boundary layer transition in wind tunnel test. In fact, the induced drag of the wind tunnel model (without separation) is generally accepted as being representative of the full scale induced drag1, indicating it is unnecessary to correct induce drag for Reynolds number effect. So the pressure distribution, boundary layer thickness and drag polar curve should be similar between wind tunnel model and flight conditions. Therefore, it is extremely important to determine transition location in wind tunnel test because the transition location affects aerodynamic characteristics obviously.

The supercritical airfoils were first designed in the 1960s, by NASA engineer Richard Whitcom2-3. A significant research effort has been emphasized on its improvement. The superior per formance enables its widely application to some civil aircrafts, such as A320, A330, A380, B77 7, and B787 and so on. Supercritical airfoils are characterized by their flatted upper surface(sucti on side surface),highly cambered aft section, an d greater leading edge radius compared with con ventional airfoil shapes. Flows about supercritic al airfoil are shown to be particularly sensitive t o viscosity.

Thus, transition location plays a significant role on aerodynamic characteristics of supercrit ical airfoils. LyndellS. King numerically studied the influence of transition location on aerodyna mic characteristics of supercritical airfoils 4.The numerical results indicated that transition locati on and extent has obvious influence on lift-to-dr ag characteris-tics, shock wave location and sub sequent boundary layer separation in transonic f low regime. Chen Yingchun stud-ied the influen ce of transition location on supercritical airfoils pressure distribution by numerical simulations a nd wind tunnel test, analyzing the pressure fluct uations in wind tunnel test5. DENNIS W BART LETT claimed that a given transition location o nly supplied appropriate simulation within limit ed range, it caused over or inadequate transition if deviating from applicable conditions substanti ally6. Over transition leaded to increase turbule nce boundary layer thickness and more extra dra g from transition trips, and inadequate transition leaded to rearward transition location. ELSTN AAR A gave the influence of over or inadequate transition on aerodynamic characteristics7.Wei Wenjian studied the differences between free an d fixed transition on drag of a small aspect ratio supercritical wing in wind tunnel test and conclu ded that it can obtain accurate test data by free tr ansition towards this small aspect ratio supercrit ical wing8.

The purpose of this study is to assess the ef fect of fixed transition location on a large aspect ratio supercritical wing by numerical simulatio n. To validate numerical simulation, we compar e simulation results with European Tran-sonic Wind tunnel (ETW) test data9. The emphasis is on the impact of the fixed transition location on pressure distri-bution, boundary layer thickness and lift-to-drag characteristics to give some guid ance for the determination of fixed transition loc ation in wind tunnel test, and then to effectively extrapolate wind tunnel test data to flight condi-tions.

2 Computational methodology

2.1 Governing equation

2.1.1 Full-potential equation

The unsteady full-potential equation written in a body fitted coordinate system is given by

$$(\rho \boldsymbol{J})_\tau + (\rho U \boldsymbol{J})_\xi + (\rho V \boldsymbol{J})_\eta + (\rho W \boldsymbol{J})_\zeta = 0 \qquad (1)$$

where ρ is density, U, V, and W are the contrav ariant velocity components in the ξ, η, and ζ, di rections, τ means time, and J is Jacobian. Eq. (1) is solved by the time-accurate approximate fact orization algorithm and internal Newton iteratio ns; body conditions and wake conditions are im plicit embedded.

2.1.2 Boundary layer equation

The original system of differential equations, w hich governs the gas flow in the three-dimensio nal boundary layer has the form:

$$\left.\begin{aligned}
&\frac{\partial}{\partial x}(\rho u h_2 \sin\theta) + \frac{\partial}{\partial z}(\rho w h_1 \sin\theta) + \frac{\partial}{\partial y}(\overline{\rho v} h_1 h_2 \sin\theta) = 0 \\
&\rho \frac{u}{h_1}\frac{\partial u}{\partial x} + \rho \frac{w}{h_2}\frac{\partial u}{\partial z} + \overline{\rho v}\frac{\partial u}{\partial y} - \rho k_1 u^2 \cot\theta + \rho k_2 w^2 \csc\theta + \rho k_{12} u w = \\
&\qquad = -\frac{\csc^2\theta}{h_1}\frac{\partial p}{\partial x} + \frac{\csc\theta\cot\theta}{h_2}\frac{\partial p}{\partial z} + \frac{\partial}{\partial y}\left(\mu\frac{\partial u}{\partial y} - \overline{\rho u' v'}\right) \\
&\rho \frac{u}{h_1}\frac{\partial w}{\partial x} + \rho \frac{w}{h_2}\frac{\partial w}{\partial z} + \overline{\rho v}\frac{\partial w}{\partial y} - \rho k_2 w^2 \cot\theta + \rho k_1 u^2 \csc\theta + \rho k_{21} u w = \\
&\qquad = -\frac{\cot\theta\csc\theta}{h_1}\frac{\partial p}{\partial x} + \frac{\csc^2\theta}{h_2}\frac{\partial p}{\partial z} + \frac{\partial}{\partial y}\left(\mu\frac{\partial w}{\partial y} - \overline{\rho w' v'}\right)
\end{aligned}\right\} \qquad (2)$$

where $\overline{\rho v} = \rho v + \overline{\rho' v'}$.

The coordinate y is directed along the normal to the wing surface, the variables x, z govern the sy stem of non-orthogonal coordinates with angle $\theta(x,z)$ between them on the surface, u,v,w - are the components of the velocity vector along the coordinates x,y,z, ρ- is the density, p - is the pressure, μ - is the dynamic viscosity coefficient, $h_1 = \partial s_1/\partial x, h_2 = \partial s_2/\partial x$ are the metric coefficients.

The parameters k_1, k_2, k_{12}, k_{21} characterize curvature of coordinate lines z=const, x=const. has form:

$$k_1 = \frac{1}{h_1 h_2 \sin\theta}\left[\frac{\partial}{\partial x}(h_2\cos\theta) - \frac{\partial h_1}{\partial z}\right]$$

$$k_2 = \frac{1}{h_1 h_2 \sin\theta}\left[\frac{\partial}{\partial z}(h_1\cos\theta) - \frac{\partial h_2}{\partial x}\right]$$

$$k_{12} = \frac{1}{\sin\theta}\left[-\left(k_1 + \frac{1}{h_1}\frac{\partial\theta}{\partial x}\right) + \cos\theta\left(k_2 + \frac{1}{h_2}\frac{\partial\theta}{\partial z}\right)\right]$$

$$k_{21} = \frac{1}{\sin\theta}\left[-\left(k_2 + \frac{1}{h_2}\frac{\partial\theta}{\partial z}\right) + \cos\theta\left(k_1 + \frac{1}{h_1}\frac{\partial\theta}{\partial x}\right)\right]$$

The boundary conditions are as follows:

on the external edge of the boundary layer:

$$y = \delta,\quad u = u_e(x,z),\quad w = w_e(x,z)$$

on the wall:

$$y = 0,\quad u = w = 0 \quad v_w = 0$$

2.2 Viscous-inviscid interaction

For the determination of self-consistent solutions the quasi-simultaneous coupling scheme is used. It allows one to take into account the expected boundary layer response to the chordwise velocity variation while calculating the external flow, and ensures effective and rapid computation of viscid-inviscid interaction including moderate separation regimes.

3 Computational validation

To validate the flowfield computation method, the DLR-F6 model was numerically simulated and compared with the experimental data at CL=0.57. The DLR-F6 model is a twin-engine aircraft model, with a variety of wind-tunnel experiment data and numerical solutions available over years. The nacelle of DLR-F6 is a through flow nacelle. Fig. 1 shows the variation of CL with the number of grid points for the DLR-F6 wing-body/nacelle, indicating that the 600000 grid points are adequate for this simulation. The computational grid for the DLR-F6 wing-body/nacelle (600000 grid points) is presented in Fig. 2.

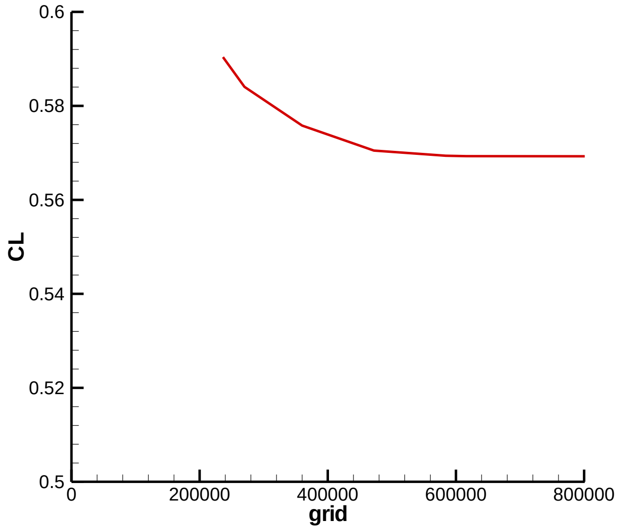

Fig. 1 The variation of CL with the number of grid points.

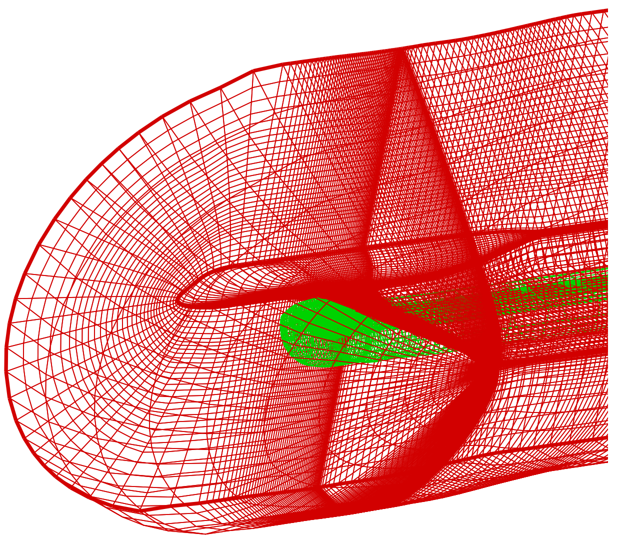

Fig. 2 DLR-F6 wing-body/nacelle grid.

The wing pressure distributions from the present computation and experiments are shown i n Fig. 3, respectively, with Ma=0.75, CL= 0.4 and Reynolds number of 3×106 based on the mean aerodynamic chord. The lift-to-drag characteristics between the calculations and experiments are shown in Fig. 4.The simulated results are in excellent agreement with the experiments, showing that the grid generation strategy and numerical method are adequate for this case. Thus, overall, the simulation gives a satisfactory prediction of pressure distribution, lift-to-drag characteristics and is therefore considered to be a satisfactory basis for determining simulations.

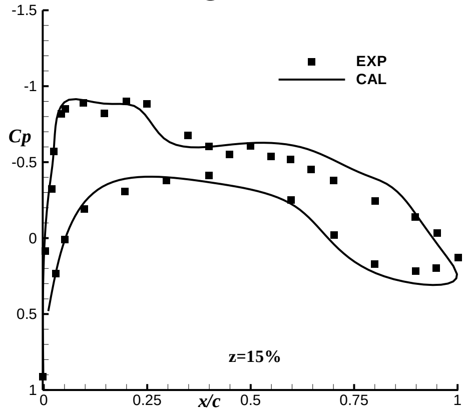

(a) at z=15%

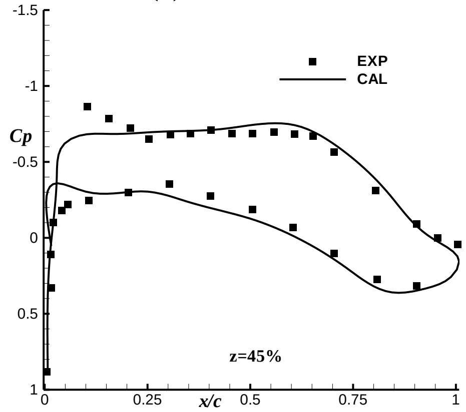

(b) at z=45%

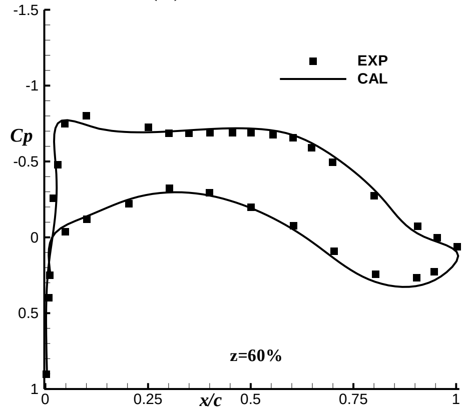

(c) at z=60%

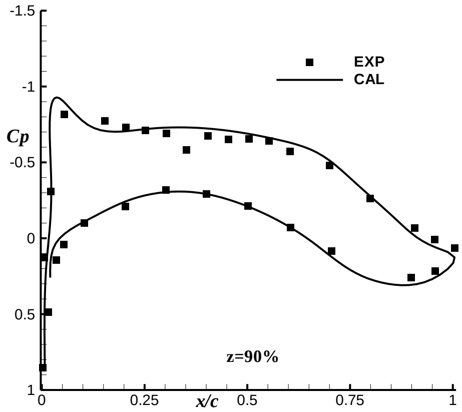

(d) at z=90%

Fig. 3 Wing surface Cp comparison at Ma=0.75.

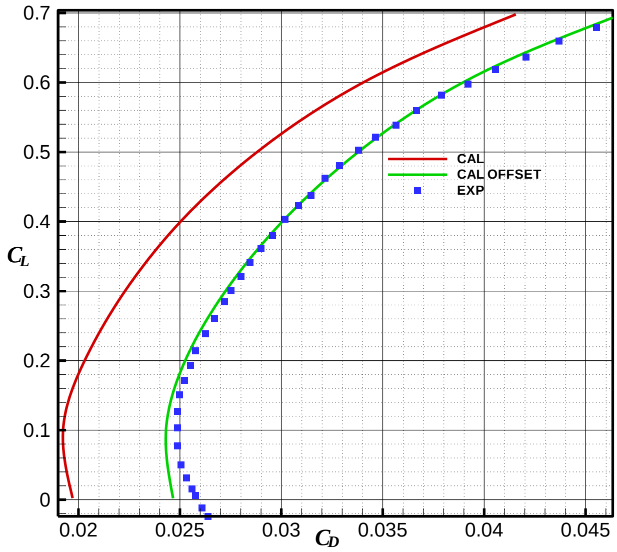

Fig. 4 Lift-to-drag characteristics comparison at Ma=0.75.

4 Results and discussion

Taking a large aspect ratio supercritical wing for instance, a numerical simulation is performed. Comparison analysis is conducted on the wind tunnel Reynolds number of 2×106,4×106,4×106 and flight Reynolds number of 24×106 based on mean aerodynamic chord at different transition location. All the following comparisons of drag polar curves are undertaken by offsetting the curves of wind tunnel Reynolds number to the one of flight Reynolds number at CL= 0.2.

4.1 Effects of fixed transition location in different Reynolds number

For the determination of self-consistent solutions the quasi-simultaneous coupling scheme is used. It allows one to take into account the expected boundary layer response to the chordwise velocity variation while calculating the external flow, and ensures effective and rapid computation of viscid-inviscid interaction including moderate separation regimes.

4.1.1 Reynolds number of 2×10^6

The numerical results for wind tunnel Reynolds number of 2×10^6 at Ma=0.785, Xtr=0.02/0.07/0.15/0.20 and flight Reynolds number of 24×10^6 at Ma=0.785, Xtr=0.02 are presented in Fig. 5. Shown in Fig. 5(a) are the wing surface pressure distributions for several transition locations at wing spanwise location of 75%. As can be seen, transition location makes appreciable difference in the shock wave location, shock wave intensity and rear loading. Note that forward transition location results in the loss of rear loading which is the typical characteristics of supercritical airfoil. For a given lift coefficient the loss of rear loading has to be compensated by increasing load on the upper surface upstream of the shock wave, with the consequence that wave drag increases with lift coefficient. Boundary layer thickness results are presented in Fig. 5(b) showing obvious differences between wind tunnel Reynolds number of 2×10^6 at Xtr =0.02/0.07/0.15/0.20 and flight Reynolds number of 24×10^6 at Xtr =0.02.This is an expected result, since, at a given transition location, delayed transition location would result in a thinner boundary layer and thus, a more rear loading in the vicinity of the trailing edge. Skin friction results for several transition locations are showed in Fig. 5(c). Note that delayed transition location results in an overshoot of the turbulent skin friction above that resulting from earlier transition location, since delayed transition location would result in a thinner boundary layer and, thus, a higher velocity gradient at the wall. Fig. 5(d) presents the drag polar curves about these lift-to-drag characteristics. In this case, there are obvious differences on the drag polar-stretching part, especially at high lift coefficient, failing to acquire reliable wind tunnel test data for the Reynolds number effect correction. So it cannot predict the flight aerodynamic characteristics under the condition of wind tunnel Reynolds number of 2×10^6 at Xtr=0.02/0.07/0.15/0.20. Consequently, the free transition test is more suitable at Reynolds number of 2×10^6.

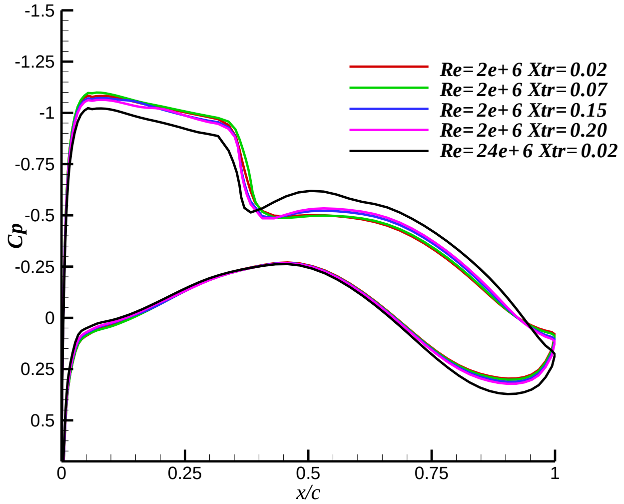

(a) Wing surface Cp at CL=0.55

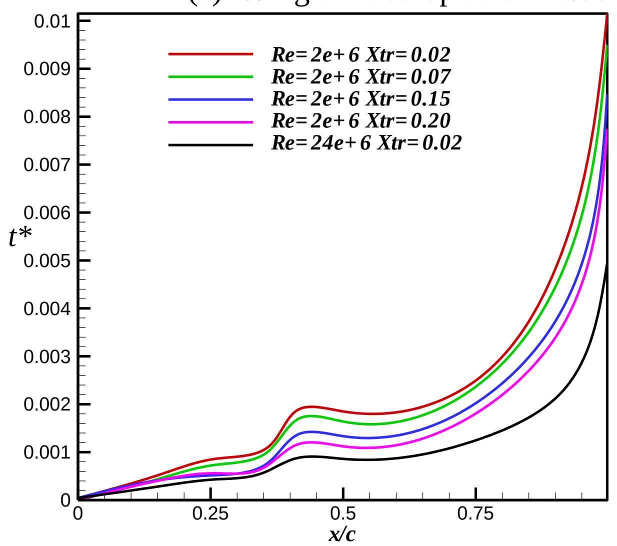

(b) Boundary layer thickness at CL=0.55

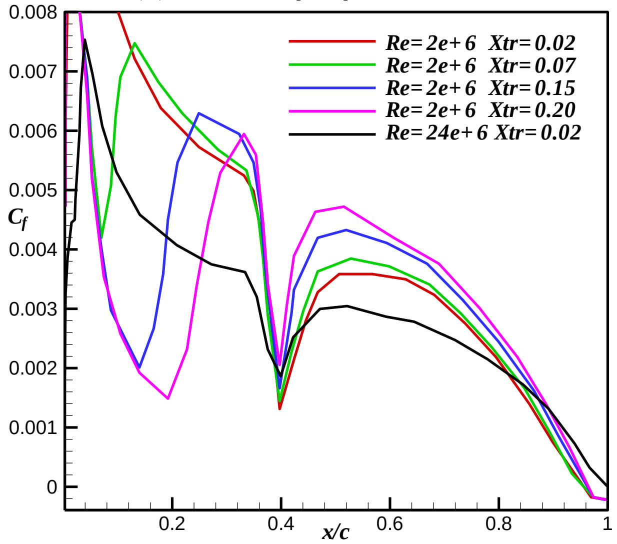

(c) Effect of transition on skin friction

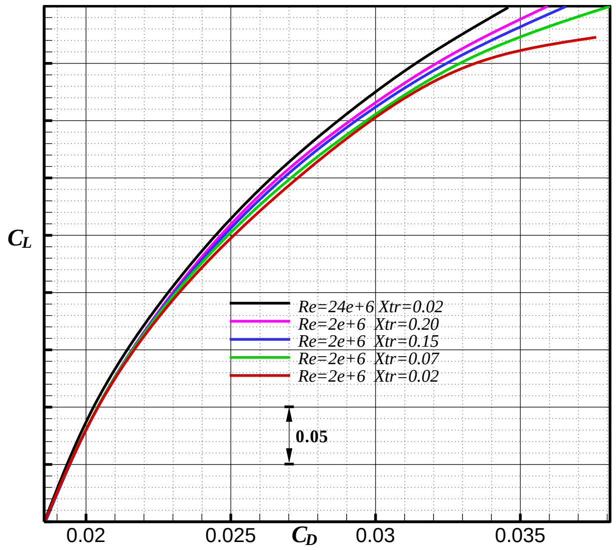

(d) Lift-to-drag characteristics comparison

Fig. 5 Aerodynamics comparison at Ma=0.785, Re=2×10^6 in different transition locations.

4.1.2 Reynolds number of 4×10^6

Also shown in Fig. 6 are the comparison of wind tunnel Reynolds number of 4×10^6 at Ma=0.785, Xtr=0.02/0.07/0.15/0.20 and flight Reynolds number of 24×10^6 at Ma=0.785, Xtr=0.02 by numerical simulation. The results of the pressure distribution, boundary layer thickness and lift-to-drag characteristics clearly show obvious differences between wind tunnel Reynolds number of 4×10^6at Xtr=0.02/0.07and flight Reynolds number of 24×10^6 at Xtr=0.02.The pressure distribution differ considerably, but their agreement increase gradually with the transition location increment while the rear loading is strengthened. The boundary layer thickness reduces closed to the one of flight Reynolds number as transition locations move aft. Meanwhile, the similarity of the drag polar-stretching part improves gradually.

As can be seen, the results under the condition of wind tunnel Reynolds number of 4×10^6 at Xtr=0.15/0.20 agree reasonably well with those of flight Reynolds number , especially at Xtr=0.20.So it can predict flight aerodynamic characteristics well at Re=4×10^6,Xtr=0.15/0.20 through fixed transition test.

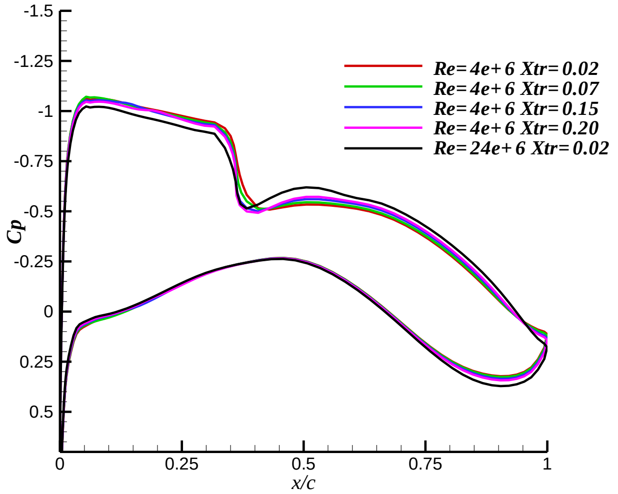

(a) Wing surface Cp at CL=0.55

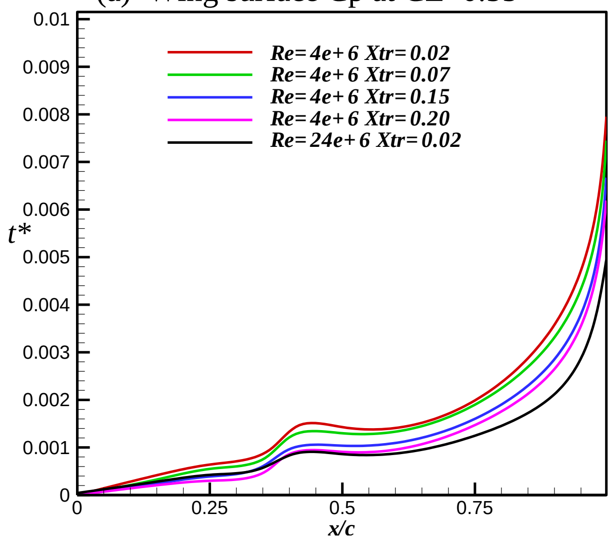

(b) Boundary layer thickness at CL=0.55

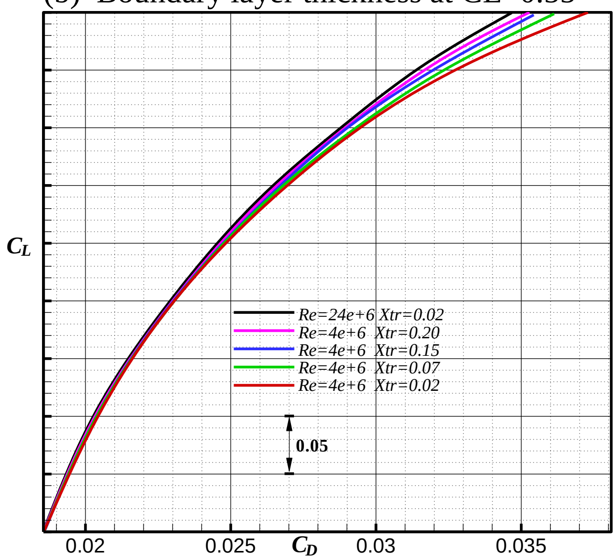

(c) Lift-to-drag characteristics comparison

Fig. 6 Aerodynamics comparison at Ma=0.785, Re=4×10^6 in different transition locations.

4.1.3 Reynolds number of 6×10^6

Fig. 7 show the comparison of wind tunnel Reynolds number of 6×10^6 at Ma=0.785, Xtr=0.02/0.07/0.15/0.20 and flight Reynolds number of 24×10^6 at Ma=0.785 ,Xtr=0.02 by numerical simulation. The results of the pressure distribution, boundary layer thickness and lift-to-drag characteristics clearly show obvious differences between wind tunnel Reynolds number of 6×10^6 at Xtr=0.02 and flight Reynolds number of 24×10^6 at Xtr =0.02.The similarity of the pressure distribution, boundary layer thickness and the drag polar-stretching part are much better under the condition of wind tunnel Reynolds number of 6×10^6 at Xtr=0.07/0.15/0.20, especially at Xtr=0.15/0.20.So it can predict flight aerodynamic characteristics well at Re=6×10^6, Xtr=0.07/0.15/0.20 through fixed transition test.

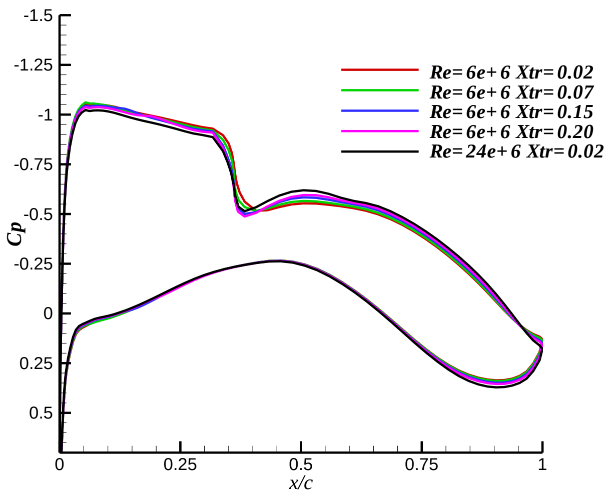

(a) Wing surface Cp at CL=0.55

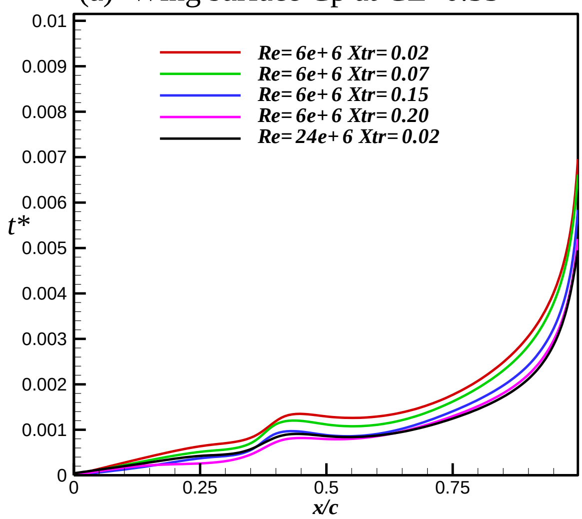

(b) Boundary layer thicknessat CL=0.55

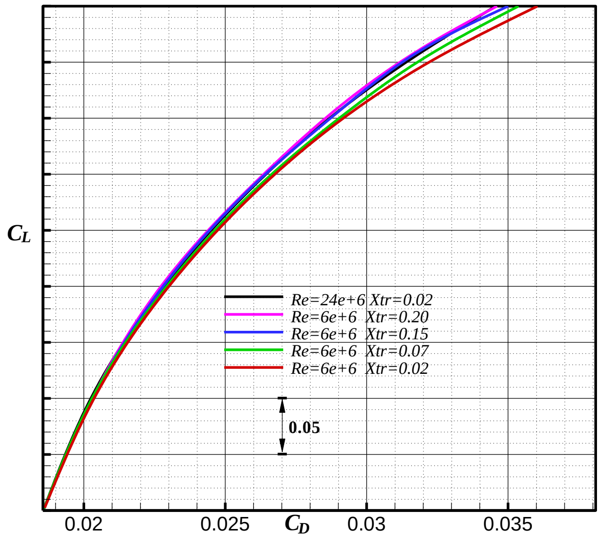

(c) Lift-to-drag characteristics comparison

Fig. 7 Aerodynamics comparison at Ma=0.785, Re=4×10^6 in different transition locations.

Above all, the results of the pressure distribution, boundary layer thickness and lift-to-drag characteristics clearly show good agreement between wind tunnel Re of 4×10^6 at Ma=0.785, Xtr=0.20, Re of 6×10^6 at Ma=0.785, Xtr=0.15/0.20 and flight Re of 24×10^6 at Ma=0.785, Xtr=0.02 within the range of attached flows. The fixed transition location can move forward to decrease aerodynamic interaction between transition trips and boundary layer when increasing Reynolds number.

4.2 Effects of fixed transition location at the different Mach number

4.2.1 The results from numerical simulations

With the aim of evaluating the effect of fixed transition location on aerodynamic characteristics at higher Mach number, a study has been made for Ma=0.82 at the fixed transition location which can predict flight aerodynamic characteristics well. Figs. 8-9 show the comparison of wind tunnel Reynolds number of 6×10^6 at Ma=0.82,Xtr=0.15/0.20 and flight Reynolds number of 24×10^6 at Ma=0.82,Xtr=0.02 by numerical simulation. There are obvious differences of shock wave location, boundary layer thickness and drag polar-stretching part at Ma =0.82 while these curves agree reasonably well at Ma =0.785. The main reason for this is that the shock wave at higher Mach number moves aft and intensifies comparing with lower Mach number, indicating that the Reynolds number effect on supercritical wing at higher Mach number becomes more obvious. The transition location which can predict flight aerodynamic characteristics well at $Re=6\times10^6$, Ma=0.785 is not suitable for that at $Re=6\times10^6$, Ma=0.82. Meanwhile the agreement at the transition location of Xtr=0.20 is a litter better than the one at Xtr=0.15.

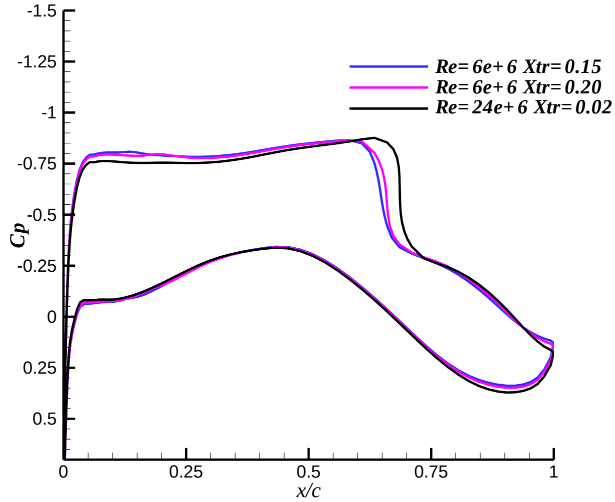

(a) Wing surface Cp comparison

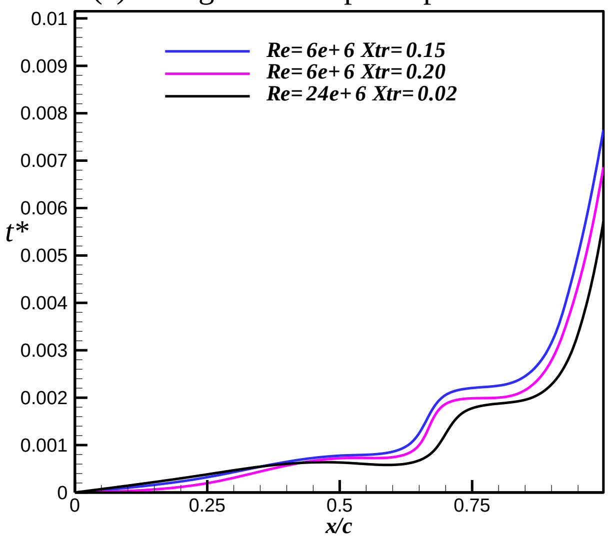

(b) Boundary layer thickness comparison

Fig. 8 Aerodynamics comparison at Ma=0.82, CL=0.5, in different transition locations.

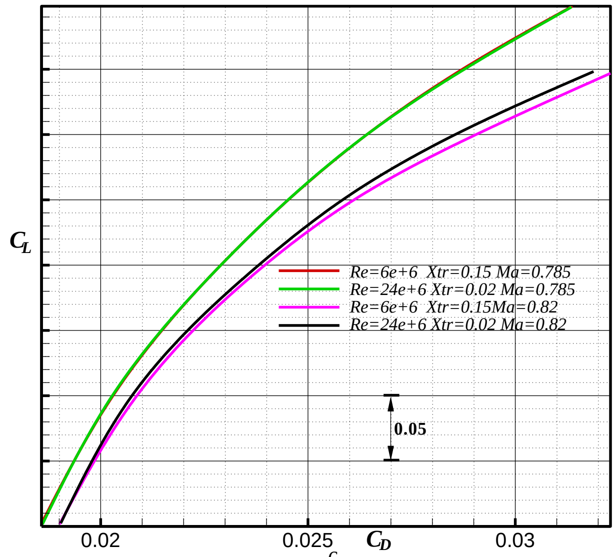

(a) $Re=6\times10^6$,Xtr=0.15

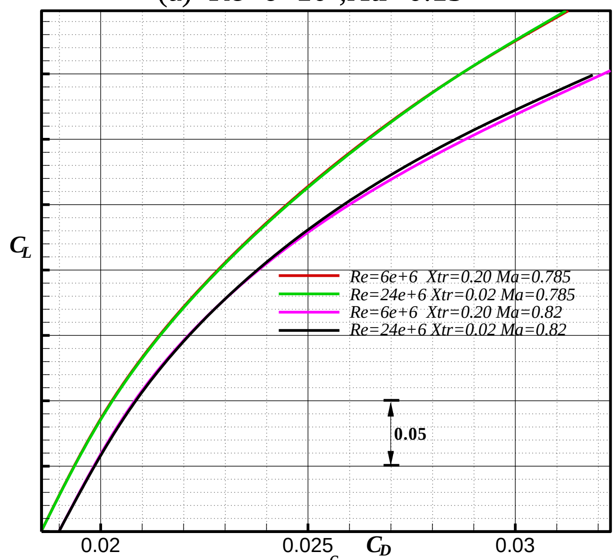

(b) $Re=6\times10^6$,Xtr=0.20

Fig. 9 Lift-to-drag characteristics comparison in the different Mach number.

4.2.2 The results from ETW test

A series of wind tunnel tests were performed at conditions equivalent to Ma=0.785 and 0.82 for the Reynolds number 4×106,6×106 and 24×106 in ETW. For the Reynolds number of 4×106,6×106 cases, the fixed transition location was Xtr=0.07,and the full scale flight case was taken to be at Re=24×106 with free transition. Fig. 10(a) highlights the comparison of drag polar curves in three different ratio of dynamic pressure to the elastic modulus. Although the aeroelastic deformation of the wing would be different in three different q/E, there are no obvious differences about drag polar curves. As a result, the data actually represents only the influence of Reynolds number. Fig. 10(b) also shows the ETW test results about the lift-to-drag characteristics at Ma=0.785, 0.82. There are greater differences between low Reynolds number and high Reynolds number at Ma=0.82 than that at Ma=0.785 according to the results. So it can come to the conclusion that the transition location at low Mach number of 0.785 is not suitable for the condition of high Mach number of 0.82, which is the same as the conclusion the numerical simulation comes to.

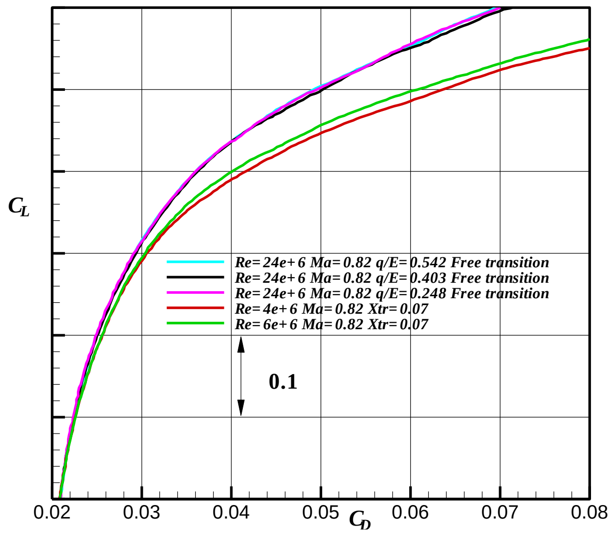

(a) The comparison in three different q/E

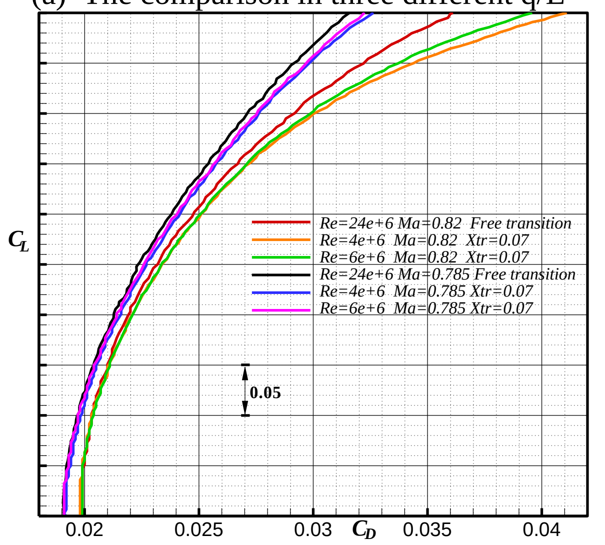

(b) The comparison between Ma=0.785 and 0.82

Fig. 10 Lift-to-drag characteristics comparison from ETW test data.

5 Conclusions

In this work, we presented the numerical simulation results of fixed transition location effects on supercritical wing aerodynamic characteristics. When several parameters (Re, CL, and Ma) were changed over a wide range, valuable results were analyzed and compared with high Reynolds number experimental data. The following conclusions were drawn.

1) The boundary layer thickness at Re=4$\times$10^6, Xtr=0.20, Ma=0.785and Re=6$\times$10^6,Xtr=0.15/0.20, Ma=0.785 are close to that of Re=24$\times$10^6, Xtr=0.02, Ma=0.785. Meanwhile, the pressure distribution and the drag polar-stretching part are similar indicating that it can properly predict the flight aerodynamic characteristics. The boundary layer thickness decreases with increased Reynolds number at the same fixed transition location. So the fixed transition location can move forward to decrease aerodynamic interaction between transition trips and boundary layer when increasing Reynolds number.

2) The fixed transition location which predicts well at lower Mach number of 0.785 is not suitable for higher Mach number of 0.82 at the same Reynolds number, indicating that the Reynolds number effect on supercritical wing at higher Mach number becomes more obvious. The differences become less when the fixed transition location moves aft.

The size of Reynolds number is required for wind tunnel test utilizing fixed transition. It fails to predict the flight aerodynamic characteristics at Re=2$\times$10^6 for the supercritical wing of this study. Therefore, the free transition test is more suitable. A given transition location only supplies appropriate simulation within limited range. So we should study the effect of fixed transition location before fixed transition test. Therefore, the results of this study can be considered as the reference for low Reynolds number wind tunnel test.

6 Contact Author Email Address

My email address: qianguangping@comac.cc

Copyright Statement